# Inhibition of Constitutively Activated Nuclear Factor-κB Induces Reactive Oxygen Species- and Iron-Dependent Cell Death in Cutaneous T-Cell Lymphoma

Michael K. Kiessling,[1] Claus D. Klemke,[2] Marcin M. Kamiński,[1] Ioanna E. Galani,[1] Peter H. Krammer,[1] and Karsten Gülow[1]

[1]Tumor Immunology Program, German Cancer Research Center (DFKZ), Heidelberg, Germany and [2]Department of Dermatology, Venereology and Allergology, University Medical Center Mannheim, Ruprecht Karl University of Heidelberg, Mannheim, Germany

## Abstract

**Aberrant signaling of the nuclear facotr (NF-κB) pathway has been identified as a mediator of survival and apoptosis resistance in leukemias and lymphomas. Here, we report that cell death of cutaneous T-cell lymphoma cell lines induced by inhibition of the NF-κB pathway is independent of caspases or classic death receptors. We found that free intracellular iron and reactive oxygen species (ROS) are the main mediators of this cell death. Antioxidants such as *N*-Acetyl-L-cysteine and glutathione or the iron chelator desferrioxamine effectively block cell death in cutaneous T-cell lymphoma cell lines or primary T cells from Sézary patients. We show that inhibition of constitutively active NF-κB causes down-regulation of ferritin heavy chain (FHC) that leads to an increase of free intracellular iron, which, in turn, induces massive generation of ROS. Furthermore, direct down-regulation of FHC by siRNA caused a ROS-dependent cell death. Finally, high concentrations of ROS induce cell death of malignant T cells. In contrast, T cells isolated from healthy donors do not display down-regulation of FHC and, therefore, do not show an increase in iron and cell death upon NF-κB inhibition. In addition, in a murine T-cell lymphoma model, we show that inhibition of NF-κB and subsequent down-regulation of FHC significantly delays tumor growth *in vivo*. Thus, our results promote FHC as a potential target for effective therapy in lymphomas with aberrant NF-κB signaling.** [Cancer Res 2009;69(6):2365–74]

## Introduction

Constitutive activation of nuclear factor κB (NF-κB) is considered to be crucial for cell survival, proliferation, and apoptosis resistance in many cancers and especially in lymphomas (1–3). In malignant cells isolated from patients with multiple myeloma (4, 5), diffuse large B-cell lymphoma (6), acute myelogenous leukemia (7), acute lymphocyte leukemia (8), chronic myelogenous leukemia (9), myelodysplastic syndrome (10, 11), and cutaneous T-cell lymphoma (CTCL; refs. 12, 13) constitutive NF-κB activation has been described. Sézary syndrome is the leukemic variant of CTCL, characterized by erythroderma, general lymphadenopathy, and Sézary cells circulating in the peripheral blood (14). It usually takes an aggressive course with a median survival time of 2 to 4 years (15). Sézary cells are malignant pleomorphic $CD4^+$ T cells, which show constitutive activation of NF-κB. Inhibition of NF-κB by IkBα overexpression results in apoptosis in these cells (12). The protective role of NF-κB in cancer cells is partially mediated by the up-regulation of antiapoptotic genes including Bcl-2 family members (1, 16). However, the involvement of these proteins in induction of apoptosis by inhibition of NF-κB was not observed. Furthermore, autophagy or release of apoptosis-inducing factor were not found to be essential for this cell death (11). Recent studies indicate that stimulation of the NF-κB pathway by tumor necrosis factor α (TNFα) activates the antioxidative defense by up-regulation of MnSOD or ferritin heavy chain (FHC; refs. 17, 18). However, whether the antioxidative defense is regulated by constitutively activated NF-κB and whether this regulation is important for cell death and survival of cancer cells is unknown.

One of the enzymes reported to be regulated by NF-κB is FHC. Ferritin is a highly conserved and ubiquitously expressed iron storage protein that consists of two subunits, the FHC and the ferritin light chain (19). Twenty-four of these subunits assemble to store up to 4,500 iron atoms (19). FHC possesses a ferroxidase activity, which converts toxic $Fe^{2+}$ into nontoxic $Fe^{3+}$, whereas ferritin light chain plays a role in iron nucleation and protein stability. Iron can participate in the Fenton reaction generating hydroxide anions and hydroxyl radicals from hydrogen peroxide ($Fe^{2+} + H_2O_2 \rightarrow Fe^{3+} + OH^- + \cdot OH$; ref. 19). Hydroxyl radicals are highly reactive molecules. They can oxidize proteins and lipids thereby generating new reactive species that induce damage to other biomolecules in a chain reaction such as fashion (20). Therefore, the proper sequestration of intracellular iron is highly critical to avoid generation of oxidative stress, and thus, homozygous deletion of FHC in mice is lethal (21). However, a small amount of free cytosolic iron—the so-called labile iron pool (LIP)—is tolerated by the cell. Thus, the uptake and sequestration of iron is tightly regulated by iron regulatory proteins, which bind to iron responsive elements of ferritin mRNA at the 5′ untranslated region (5′UTR) and block translation (22). In the presence of high cellular concentrations of iron, the iron responsive element binding activity of iron regulatory protein is diminished and translation is derepressed (22). Consequently, overexpression of FHC results in down-regulation of LIP (23, 24) and lower levels of reactive oxygen species (ROS; refs. 24, 25).

Here, we report that inhibition of the NF-κB pathway by specific inhibitors cause an iron- and ROS-dependent, but caspase- and cathepsin-independent, cell death of CTCL cell lines and of primary

**Note:** Supplementary data for this article are available at Cancer Research Online (http://cancerres.aacrjournals.org/).

**Requests for reprints:** Karsten Gülow, German Cancer Research Center, Im Neuenheimer Feld 280, Heidelberg 69120, Germany. Phone: 00496221423765; Fax: 00496221411715; E-mail: k.guelow@dkfz-heidelberg.de.



doi:10.1158/0008-5472.CAN-08-3221

cells from patients with Sézary syndrome. We show that inhibition of the NF-κB signaling pathway results in induction of massive oxidative stress and cell death, which can be blocked by antioxidants such as *N*-Acetyl-L-cysteine (NAC) and glutathione mono-ethyl-ester (GSH) or the iron chelator desferrioxamine (DFO). Furthermore, inhibition of the NF-κB pathway induces an increase of free intracellular iron in CTCL cell lines and in T cells from Sézary patients but not in T cells from normal healthy donors. We show that inhibition of constitutively active NF-κB results in down-regulation of FHC in T cells from Sézary patients but not in T cells from healthy donors. Direct down-regulation of FHC by siRNA causes a ROS-dependent cell death. Finally, using a murine T-cell lymphoma model, we show that NF-κB inhibition significantly delays tumor growth *in vivo* by down-regulation of FHC. Thus, manipulation of the intracellular iron balance by targeting iron storage proteins could have a therapeutic effect on the treatment of cancer.

## Materials and Methods

**Chemicals.** NF-κB activation inhibitor (*NF-κB inh.*), cell permeable NEMO-Binding Domain Binding Peptide (NBD), cell permeable mutant NBD, DFO, and Glutathione monoethyl ester (GSH) were purchased from Merck. 2.2'-Dipyridyl Reagent Plus (DP), NAC, D-Penicillamine, Neocuproine, Manganese (III) tetrakis 4-benzoic acid porphyrin, Ebselen, and butylated hydroxyl-anisole were purchased from Sigma-Aldrich. Pancaspase inhibitor zVAD and cathepsin inhibitor Z-FA-fmk were purchased from R&D Systems. Enbrel was kindly provided by Dr. Walczak (Imperial College London, London, United Kingdom). Dichlorodihydrofluorescein-diacetate ($H_2$DCFDA) was obtained from Molecular Probes. Fe (II)-glycin-sulfat [Fe(II)] was purchased as Ferrosanol from Schwarz Pharma. The neutralizing anti-CD95L antibody Nok1 was obtained from BD Pharmingen. AnnexinV–FITC antibody was obtained from Immunotools. AnnexinV–APC antibody was obtained from BD Bioscience Pharmingen. Monoclonal Antibodies T-cell receptor Vβ1-FITC and Monoclonal Antibodies T-cell receptor Vβ2-FITC were purchased from Immunotech. CuZnSOD (SOD-1, C-17) antibody was purchased from SantaCruz. Catalase antibody was purchased from Merck.

**Quantitative reverse transcription-PCR.** Total cellular RNA was isolated using "Absolutely mRNA Purification kit" (Stratagene). Total RNA (5 μg) was reverse transcribed with a reverse transcription-PCR (RT-PCR) kit (Applied Biosystems). Quantitative RT-PCR was performed with Power SYBR Green PCR Master Mix (Applied Biosystems). Gene expression was analyzed using the 7500 Real-time PCR Systems and Sequence Detection Software version 1.2.2 (Applied Biosystems). Relative expression was determined from cycle threshold (Ct) values and was normalized using glyceraldehydes-3-phosphate dehydrogenase as the endogenous reference. Primer sequences are found in the Supplementary Materials and Methods section.

**Mice, tumor cell line, and tumor cell injection.** C57BL/6 wild-type were purchased from Charles River Laboratories. Mice were housed under specific pathogen-free conditions and used in experiments at ages 6 to 8 wk. All experiments were performed according to local animal experimental ethics committee guidelines. For the analysis of tumor growth *in vivo*, groups of 14 mice were injected s.c. in the left flank with $1 \times 10^6$ RMA-S cells in PBS. Controls (NaCl treated) received 100 μL 0.9% NaCl i.p. and mice of the NF-κB inhibitor group received 8.91 μL of NF-κB inhibitor in DMSO (5 μmol/L stock) and 91 μL 0.9% NaCl i.p. Treatment of mice started on day 6 after tumor cell injection for 2 cycles of 5 d of daily treatment with a 2-d intermission after the first cycle. Tumor growth was assessed beginning on day 5, then daily after day 7 with a caliper measuring along the perpendicular axes of the tumors and expressed as the product of the two diameters. On day 17, mice were sacrificed and tumors were removed, cut into small pieces, and digested with 5 mg/mL collagenase type 4 (Cell Systems GmbH) and 0.5 mg/mL DNase I (Sigma-Aldrich) at 37°C for 15 min. Erythrocytes were lysed by using buffered ammonium chloride solution. Blood counts were performed by the clinical laboratories of the University of Heidelberg, Germany.

**ROS generation assays.** ROS levels were assayed as described recently (26, 27). Briefly, cells were stained with the oxidation-sensitive dye $H_2$DCFDA (5 μmol/L) for 30 min. Then, cells were treated with NF-κB inhibitor or NBD for 2 h. Treatment was terminated by ice-cold PBS and ROS generation was determined by fluorescence-activated cell sorting (FACS). The increase in fluorescence of treated versus untreated samples is shown. In the case of FHC down-regulation by siRNA or preincubation with the iron chelator DFO and DP, cells were first treated with siRNA, DFO, or DP for 6 h and then stained with 5 μmol/L $H_2$DCFDA for 30 min. ROS generation was determined by FACS and quantified as the increase in mean fluorescence intensity (MFI), calculated by the following formula: increase in MFI (%) = $[(MFI_{stimulated} - MFI_{unstimulated})/MFI_{unstimulated}] \times 100$ (26).

**LIP assays.** Cells were incubated with 0.01 μmol/L calcein-AM for 5 min at 37°C in medium. Then, cells were left mock treated or treated with 20 μmol/L NF-κB inhibitor, 40 μmol/L NBD, or 0.1 μg/mL Fe (II) for 2 h. Next, each cell sample was divided into two individual samples. One sample was either left untreated as control, the other was incubated with 100 μmol/L DP for 2 h, washed with cold PBS, and fluorescence of calcein was measured at 480 nm excitation and 520 nm emission. Fe (II) and Fe (III) quench the fluorescence of calcein, which allows an estimation of LIP in cells. Addition of strong Fe (II) chelators such as DP competes for Fe (II) binding with calcein and fluorescence of calcein increases. The increase in fluorescence provides a value to estimate the previous concentration of calcein-bound iron, which corresponds to the actual LIP (23, 28). The increase in fluorescence of mock-treated cells was set to 100% and compared with the increase in fluorescence of cells treated with 20 μmol/L NF-κB inhibitor, 40 μmol/L NBD, or 0.1 μg/mL Fe (II). LIP was determined by FACS and quantified as the increase in MFI between samples not treated with DP and samples treated with DP. Increase in MFI of mock-treated cells was set to 100% and compared with the increase of MFI of NF-κB inhibitor, NBD, or Fe (II)–treated cells.

**Cell death assays.** For cell death induction, MyLa cells or peripheral T cells were stimulated with indicated concentrations of inhibitors. Cell death was assessed by forward-to-side-scatter profile (29) or by AnnexinV–FITC (Immunotools) and propidium iodide (Sigma-Aldrich). Specific cell death was calculated by the following equation: specific cell death % = (% experimental cell death − % spontaneous cell death)/(100% − % spontaneous cell death) × 100 (26, 27).

## Results

**NF-κB inhibition induces ROS-dependent cell death in T cells from Sézary patients.** We investigated the role of constitutive NF-κB activation for cell survival in Sézary syndrome. Primary T cells isolated from 12 patients suffering from Sézary syndrome were incubated with a chemical NF-κB inhibitor (30) or the NBD (31). Both inhibitors show equal efficiency to block NF-κB activation (Supplementary Fig. S1*A*). NF-κB inhibition led to a significant induction of cell death in T cells from all patients investigated but not of 12 healthy donors (Fig. 1*A*). This shows that malignant T cells are more sensitive toward inhibition of NF-κB than T cells from normal healthy donors. Treatment of T cells from Sézary patients with another NF-κB inhibitor, NBD, induced cell death compared with its inactive version cell permeable mutant NBD (Supplementary Fig. S1*B*).

Sézary cells are characterized by the expression of monoclonal Vβ chain of the T-cell receptor, which is specific for the individual patients (32). To check whether Sézary cells are more sensitive to inhibition of NF-κB than normal cells in the same patient, we isolated $V\beta^+$ and $V\beta^-$ T cells of three patients. Indeed, cell death induced by the NF-κB inhibitor of the malignant $V\beta2^+$ population is stronger than in the nonmalignant $V\beta2^-$ population (Fig. 1*B*). To

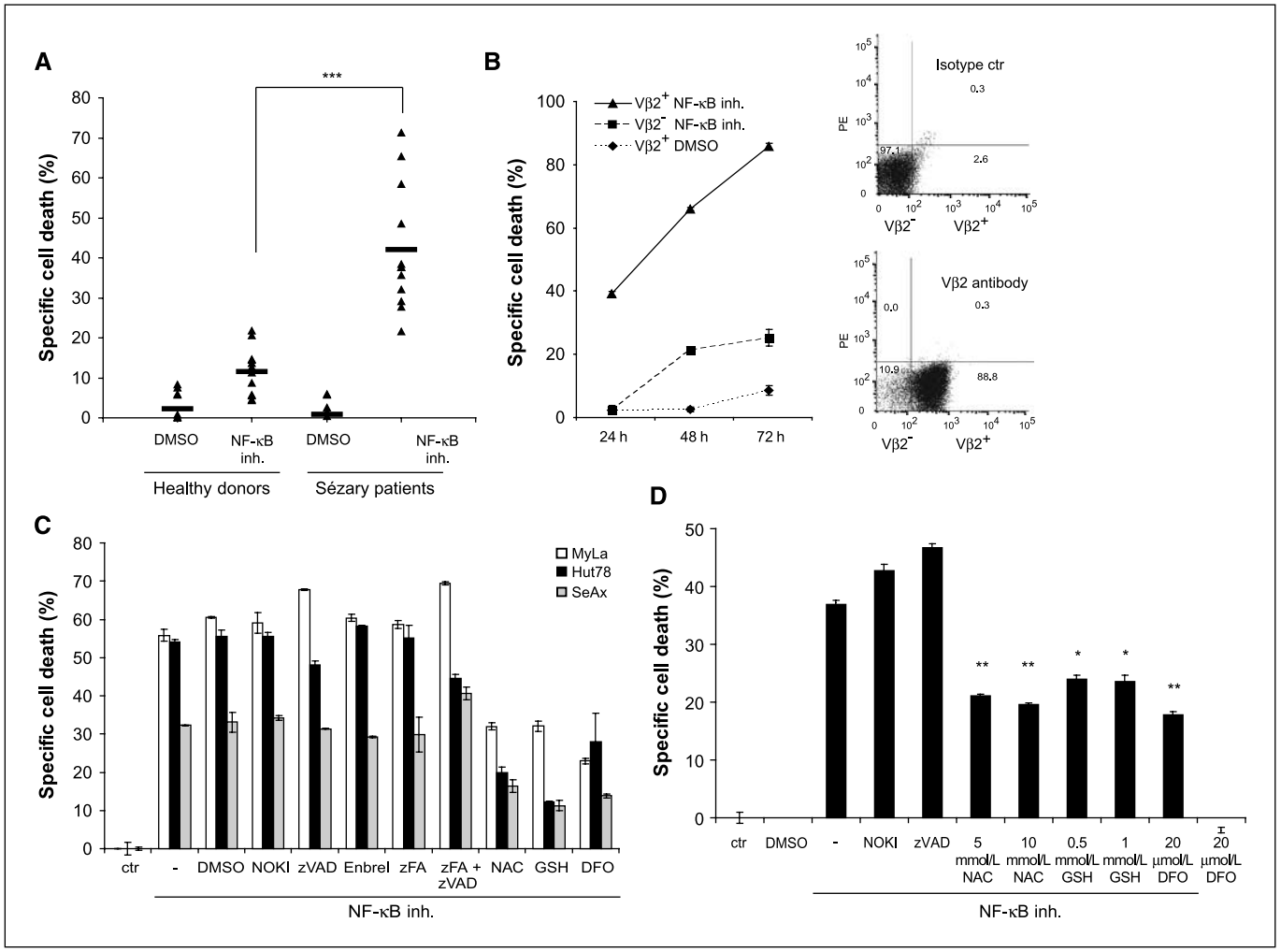


**Figure 1.** Survival of primary cells from Sézary patients and the CTCL cell lines MyLa, Hut78, and SeAx depend on constitutive NF-κB activation. *A,* purified peripheral T cells of 12 healthy donors and 12 patients with Sézary syndrome were treated with 1% DMSO or 5 μmol/L NF-κB inhibitor for 72 h. Cell death was assessed by flow cytometry. Cell death was calculated as described in Materials and Methods. Student's *t* test, $P < 0.001$ (***). *B,* malignant T cells of patient 1 were stained with a monoclonal antibody directed against the clonal region of Vβ2$^+$ T-cell receptor and sorted by flow cytometry (*top right* and *bottom*). Cells were treated with 5 μmol/L NF-κB inhibitor and cell death of Vβ2$^+$ and Vβ2$^-$ was assessed by flow cytometry (*left*). *C,* the CTCL cell lines MyLa, Hut78, and SeAx were treated with 20 μmol/L NF-κB inhibitor and cotreated with 1% DMSO, 1% NOK 1, 20 μmol/L zVAD, 25 μmol/L Enbrel, 50 μmol/L zFA, 50 μmol/L zFA and 20 μmol/L zVAD, 20 mmol/L NAC, 0.5 mmol/L GSH, or 20 μmol/L DFO for 24 and 48 h. Cell death was assessed by flow cytometry. *D,* purified peripheral T cells of a Sézary patient were treated with 5 μmol/L NF-κB inhibitor and cotreated with NAC, GSH, or DFO for 24 h. Cell death was assessed by flow cytometry. The experiment shown is representative for three independent patients analyzed. Student's *t* test, $P < 0.05$ (*); $P < 0.01$ (**). *Ctr,* control.

investigate the molecular mechanism of cell death induction by inhibition of NF-κB, we used the CTCL cell lines MyLa, Hut78, and SeAx, which can be sensitized toward cell death by NF-κB inhibitor comparable with primary Sézary cells (Fig. 1*C*). Cotreatment with a neutralizing anti-CD95 ligand (CD95L) antibody (NOK1), a pancaspase inhibitor (zVAD), a soluble TNF-Receptor-Fc (Enbrel), and a cathepsin inhibitor (zFA) did not block cell death induced by NF-κB inhibition (Fig. 1*C*). This shows that the cell death observed here is caspase independent and differs from classic cell death pathways. Remarkably, antioxidants including NAC, cell permeable GSH, or the iron chelator DFO could diminish cell death induced by the NF-κB inhibitor (Fig. 1*C*) or the NBD (Supplementary Fig. S1*C* and *D*). This implies that the generation of ROS and the release of iron are involved in cell death induced by NF-κB inhibition. A similar outcome was obtained for primary T cells from Sézary patients incubated with the NF-κB inhibitor (Fig. 1*D*). The addition of NAC, GSH, or DFO prevented cell death, whereas addition of NOK1 or zVAD did not interfere with cell death induction by NF-κB inhibitor (Fig. 1*D*). Thus, generation of ROS and the release of iron are involved in cell death by NF-κB inhibition of malignant T cells from Sézary patients.

**Inhibition of the NF-κB signaling pathway results in ROS generation and an increase of iron.** Because cell death induced by NF-κB inhibition was dependent on ROS, we next sought to determine whether NF-κB inhibition generates ROS in CTCL cell lines. Cells were incubated with the oxidation sensitive dye $H_2$DCFDA (26, 27) and incubated with the NF-κB inhibitor or with NBD for 2 h. Inhibition of NF-κB activation by NF-κB inhibitor generated a strong oxidative stress without any costimulation that could be blocked by addition of NAC or GSH (Fig. 2*A*). Similar results were obtained for NBD (Supplementary Fig. S2*A*). This indicates that constitutively active NF-κB regulates the expression of proteins or enzymes with antioxidative capacity and prevents accumulation of toxic ROS (17, 18). To analyze whether an increase

of intracellular iron is responsible for induction of oxidative stress, MyLa, Hut78, and SeAx cells were preincubated with the iron chelator DFO before application of the NF-κB inhibitor. We detected that the iron chelator DFO blocked ROS generation in all three cell lines (Fig. 2*B*), suggesting an involvement of Fenton chemistry for which $H_2O_2$ is required. To specify ROS, which is generated by inhibition of NF-κB, we overexpressed Catalase and CuZnSOD, which selectively degrade $H_2O_2$ and superoxide anion ($O_2^{\cdot-}$), respectively. Overexpression of Catalase and CuZnSOD was confirmed by Western Blot (Supplementary Fig. S2*D*). Catalase but not CuZnSOD blocked ROS generated by inhibition of NF-κB showing that $H_2O_2$ is important for the induction of ROS (Fig. 2*C*) as required for the Fenton reaction. The glutathione peroxidase mimetic ebselen or the hydroxyl radical scavenger butylated hydroxyl-anisole equally blocked ROS generation, whereas the SOD mimetic Manganese (III) tetrakis 4-benzoic acid porphyrin had no effect on ROS generation (data not shown). To further evaluate the involvement of iron homeostasis in cell death induced by inhibition of NF-κB, we investigated the level of free intracellular iron, the so-called LIP, upon NF-κB inhibitor treatment. In comparison to untreated control cells, MyLa, Hut78, and SeAx cells treated with the NF-κB inhibitor showed an increase of LIP of ~60% to 70% (Fig. 2*D*). As an internal control, 0.1 μg/mL of $Fe^{2+}$ was added to MyLa cells, which caused a similar increase of LIP

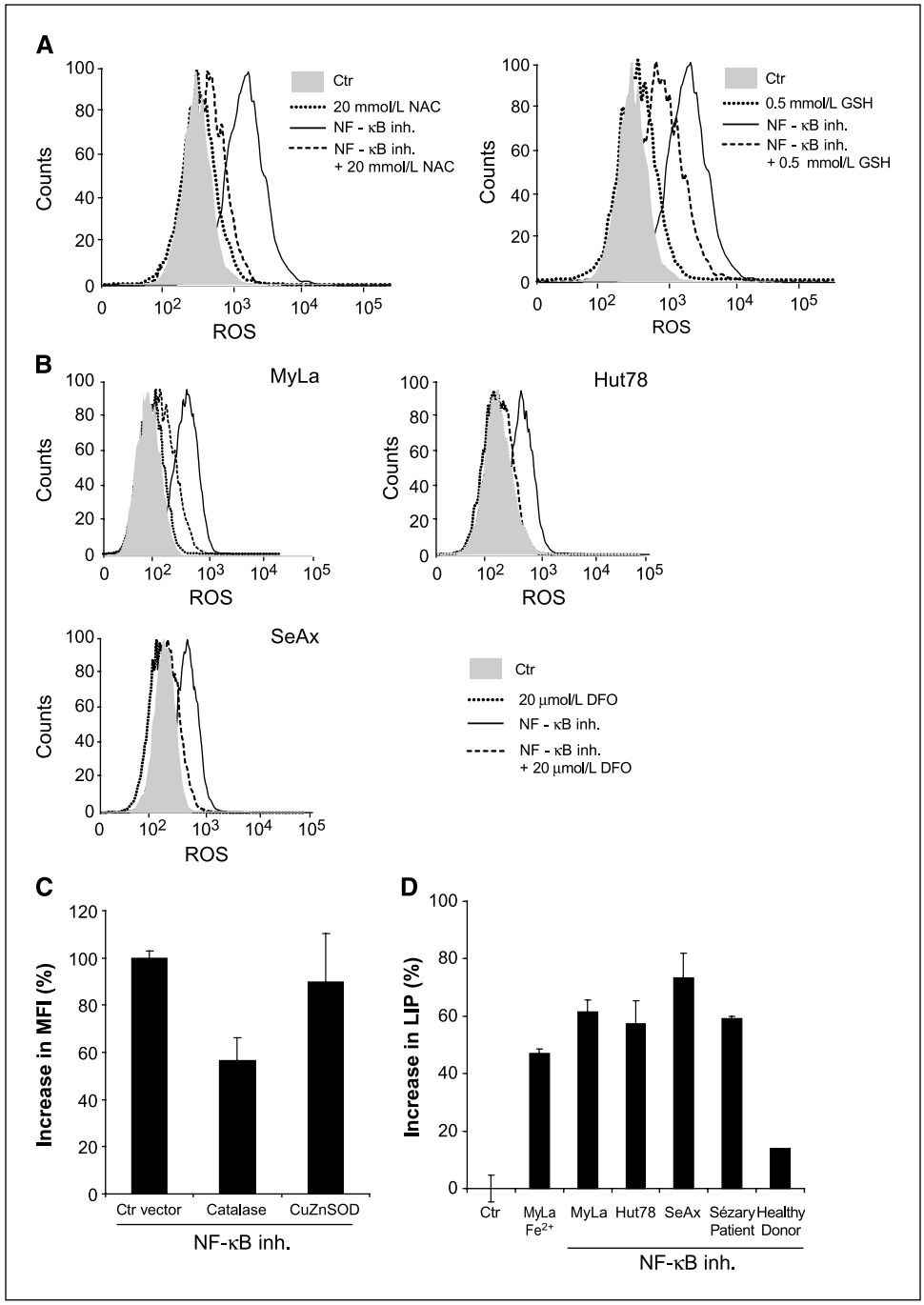


**Figure 2.** NF-κB inhibitor induces ROS and release of iron in CTCL cell lines. *A*, MyLa cells were preincubated with $H_2$DCFDA for 30 min, next preincubated with the indicated concentrations of NAC (*left*) or GSH (*right*) for 30 min. Then, cells were treated with 20 μmol/L NF-κB inhibitor for 2 h and fluorescence was detected by flow cytometry. *B,* CTCL cell lines MyLa, Hut78, and SeAx were preincubated with 20 μmol/L DFO for 6 h. Then 5 μmol/L $H_2$DCFDA were added for 30 min. Next, samples were treated with 20 μmol/L NF-κB inhibitor for 2 h and fluorescence was detected by flow cytometry at fluorescence of 518 nm. *C,* Myla cells were transiently transfected with control vector, a vector encoding catalase, and a vector encoding CuZnSOD. Then, cells were stained with $H_2$DCFDA for 30 min and treated with 20 μmol/L NF-κB inhibitor for 2 h. Fluorescence was detected by flow cytometry. The increase in MFI was normalized to untreated samples. *D,* MyLa, Hut78, SeAx cell lines, purified T cells from three Sézary Patients, and purified T cells from three healthy donors were investigated for release of iron after treatment with NF-κB inhibitor. Cells were incubated with 0.01 μmol/L calcein-AM for 30 min, either left untreated or stimulated with NF-κB inhibitor for 2 h or with 0.1 μg/mL of $Fe^{2+}$. Then, all samples were treated with 100 μmol/L DP for 1 h. Fluorescence of calcein was measured. The increase in MFI was calculated as described in Materials and Methods and is related to free intracellular iron. Untreated cells were normalized to 100%.

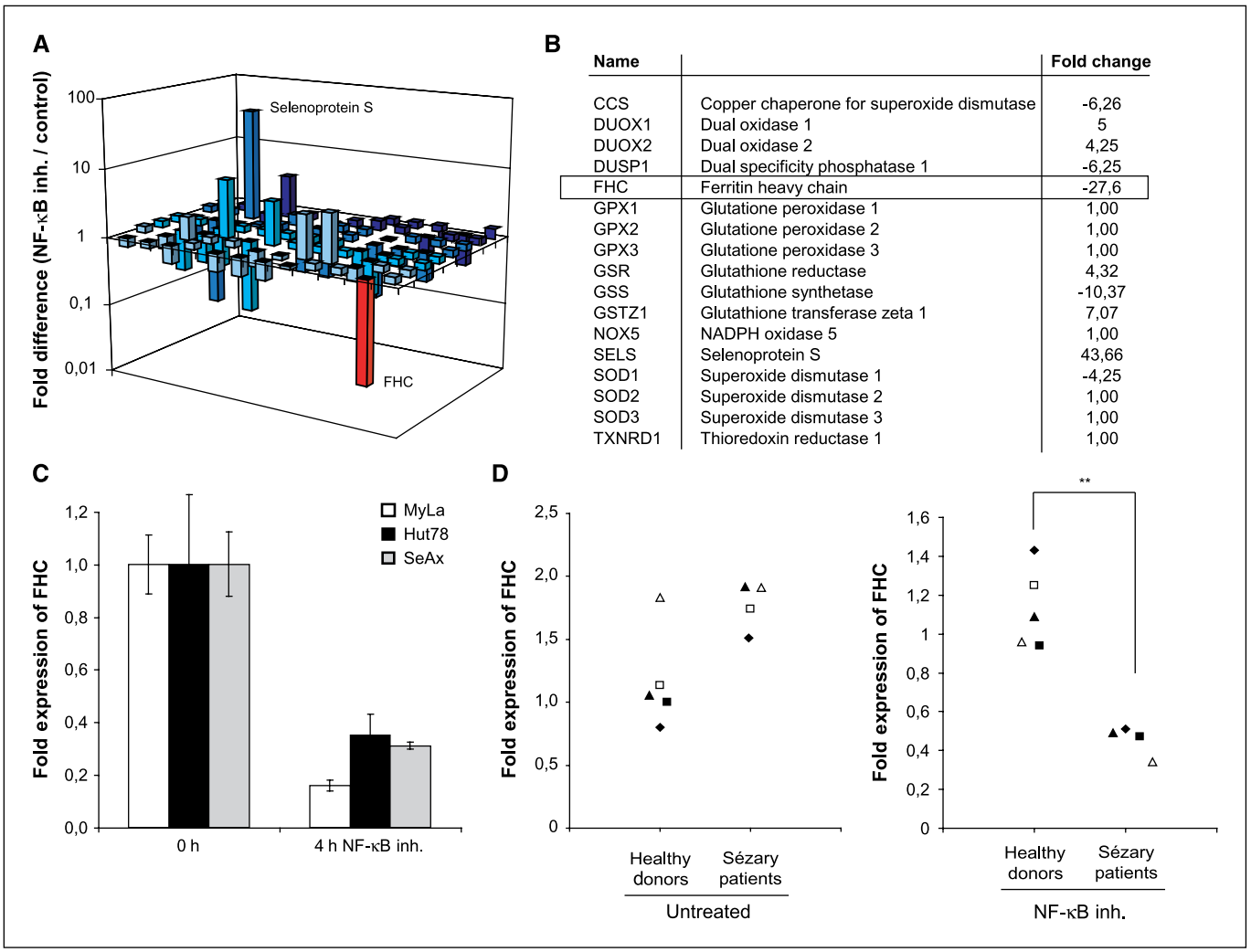


| Name | | Fold change |
|---|---|---|
| CCS | Copper chaperone for superoxide dismutase | -6,26 |
| DUOX1 | Dual oxidase 1 | 5 |
| DUOX2 | Dual oxidase 2 | 4,25 |
| DUSP1 | Dual specificity phosphatase 1 | -6,25 |
| FHC | Ferritin heavy chain | -27,6 |
| GPX1 | Glutatione peroxidase 1 | 1,00 |
| GPX2 | Glutatione peroxidase 2 | 1,00 |
| GPX3 | Glutatione peroxidase 3 | 1,00 |
| GSR | Glutathione reductase | 4,32 |
| GSS | Glutathione synthetase | -10,37 |
| GSTZ1 | Glutathione transferase zeta 1 | 7,07 |
| NOX5 | NADPH oxidase 5 | 1,00 |
| SELS | Selenoprotein S | 43,66 |
| SOD1 | Superoxide dismutase 1 | -4,25 |
| SOD2 | Superoxide dismutase 2 | 1,00 |
| SOD3 | Superoxide dismutase 3 | 1,00 |
| TXNRD1 | Thioredoxin reductase 1 | 1,00 |

**Figure 3.** NF-κB inhibitor induces down-regulation of FHC in CTCL cell lines and T cells isolated from Sézary patients. *A* and *B,* expression of genes involved in oxidative stress and antioxidative defense were evaluated by quantitative RT-PCR ($RT^2$ Profiler PCR Array system). MyLa cells were either left untreated or treated with 20 μmol/L NF-κB inhibitor for 4 h. Relative changes of selected genes of untreated to NF-κB inhibitor–treated cells are shown. *C,* CTCL cell lines MyLa, Hut78, and SeAx were treated with 20 μmol/L NF-κB inhibitor for 4 h and expression of FHC was evaluated by quantitative RT-PCR. *D,* the relative expression levels of FHC in untreated T cells from four Sézary patients and T cells from five healthy donors of comparable age were validated by quantitative RT-PCR (*left*). Then, T cells of these donors were incubated with 5 μmol/L NF-κB inhibitor for 4 h and the expression level of FHC was validated by quantitative RT-PCR (*right*). Expression levels of NF-κB inhibitor–treated samples were normalized to untreated samples. Student's *t* test, $P < 0.01$ (**).

(Fig. 2*C*). Remarkably, Sézary cells from three patients showed a similar increase of LIP to CTCL cell lines, whereas healthy donors did not show a significant increase (Fig. 2*C*). This reflects that inhibition of NF-κB has a severer effect on Sézary cells in which NF-κB is constitutively activated than on cells of normal healthy donors without constitutive activation of NF-κB. In conclusion, inhibition of NF-κB results in an increase of intracellular iron in cells with otherwise constitutive activation of NF-κB that leads to strong generation of ROS.

**Inhibition of the NF-κB signaling pathway results in down-regulation of FHC.** The NF-κB pathway has been reported to regulate the expression of proteins or enzymes with antioxidative capacities that prevent accumulation of toxic ROS (17, 18). Therefore, we decided to analyze 84 genes that were previously described to be involved in the antioxidative defense by quantitative RT-PCR upon NF-κB inhibition (33, 34). The antioxidative defense is a complex network controlled by many different means. We observed up-regulation of antioxidative enzymes such as glutathione reductase or glutathione transferase ζ 1, indicating that cells respond to the disturbance of the redox equilibrium via up-regulation of antioxidative enzymes, which are most probably not under control of NF-κB (Fig. 3*A* and *B*). This up-regulation seems to be inefficient or too late to protect cells because the net result is an increase in ROS and cell death (Figs. 1 and 2). In addition, we found several antioxidative genes, including the copper chaperone for superoxide dismutase and glutathione synthetase, which were down-regulated upon incubation of MyLa cells with the NF-κB inhibitor (Fig. 3*A* and *B*). However, the strongest decrease in mRNA expression (−27-fold) was observed for FHC (Fig. 3*A* and *B*). FHC has been described as target for NF-κB upon TNFα stimulation in fibroblasts (18). However, here, we found that FHC is a target for constitutive NF-κB signaling in malignant lymphomas without additional stimuli. Furthermore, we treated Hut78 and SeAx cells with the NF-κB inhibitor and observed a down-regulation of FHC in these cell lines (Fig. 3*C*). Therefore, these results suggest a crucial role for FHC

in cell death induced by NF-κB inhibition. To check whether constitutively activated NF-κB regulates FHC in malignant cells, T cells from patients suffering from Sézary syndrome were treated with the NF-κB inhibitor. Interestingly, a significant down-regulation of FHC mRNA levels in T cells from Sézary patients was observed, whereas FHC mRNA was not down-regulated in T cells from healthy donors (Fig. 3*D, right*). The relative expression levels of FHC were found to be higher in T cells from Sézary patients than in T cells from healthy donors (Fig. 3*D, left*). Thus, this shows that constitutively active NF-κB regulates FHC expression in malignant T cells from Sézary patients.

**Down-regulation of FHC by siRNA induces cell death.** To test whether FHC down-regulation and consecutive ROS induction is the mechanism responsible for cell death induction by NF-κB inhibition, we directly down-regulated FHC expression in MyLa cells by specific siRNAs. siRNA-mediated knockdown of FHC by four different siRNAs decreased expression of FHC mRNA up to 70% (Fig. 4*A*). Down-regulation of FHC expression by these siRNAs resulted in induction of cell death (Fig. 4*B*), whereas viability of nonsense siRNA treated cells was >80% (data not shown). Cell death was not induced by nonsense siRNA and one siRNA targeted against MAP kinase kinase 4, a protein not involved in NF-κB signaling. To further ensure that cell death is mediated by down-regulation of FHC, we down-regulated endogenous FHC by an siRNA targeting the 3′UTR of FHC and rescued cell viability by transient overexpression of FHC, which is not affected by siRNA treatment (Fig. 4*C*). Therefore, exogenous FHC restored cell viability showing that cell death was specifically caused by down-regulation of FHC. Furthermore, we investigated whether down-regulation of FHC is lethal for malignant $V\beta^+$ T cells from patients. siRNA-mediated knockdown of FHC by siRNAs decreased expression of FHC mRNA up to 50% in primary cells from Sézary patients (Fig. 4*D, insert*). Indeed, down-regulation of FHC expression induced up to 20% cell death of $V\beta^+$ T cells isolated from Sézary patients (Fig. 4*D*), whereas viability of cells treated with nonsense siRNA was >85% (data not shown). These results show that down-regulation of FHC is lethal for cell lines and primary tumor cells.

**Down-regulation of FHC by siRNA leads to generation of oxidative stress.** Because ROS seems to be a major mediator of cell death induced by NF-κB inhibitors, we analyzed whether down-regulation of FHC expression by siRNA also results in ROS generation. Reduced expression of FHC led to increased ROS production compared with treatment with nonsense or MAP kinase kinase 4 siRNA (Fig. 5*A*). The increase of ROS observed was comparable with ROS generation induced by application of the NF-κB inhibitor (Fig. 2*A*). In addition, induction of ROS upon down-regulation of FHC expression by siRNA was observed in malignant T cells from Sézary patients (Fig. 5*B*). Furthermore, we found that cell death induced by down-regulation of FHC expression was dependent on ROS because the antioxidants NAC and GSH could efficiently inhibit cell death (Fig. 5*C*). These findings show that down-regulation of FHC expression causes generation of ROS and, subsequently, cell death. To further delineate the role of FHC, we decided to transiently overexpress FHC in MyLa cells and to analyze cell death. As expected, cells overexpressing FHC showed decreased sensitivity toward the NF-κB inhibitor or NBD (Fig. 5*D*). This shows that toxicity of NF-κB inhibitors are mediated by down-regulation of FHC. Thus,

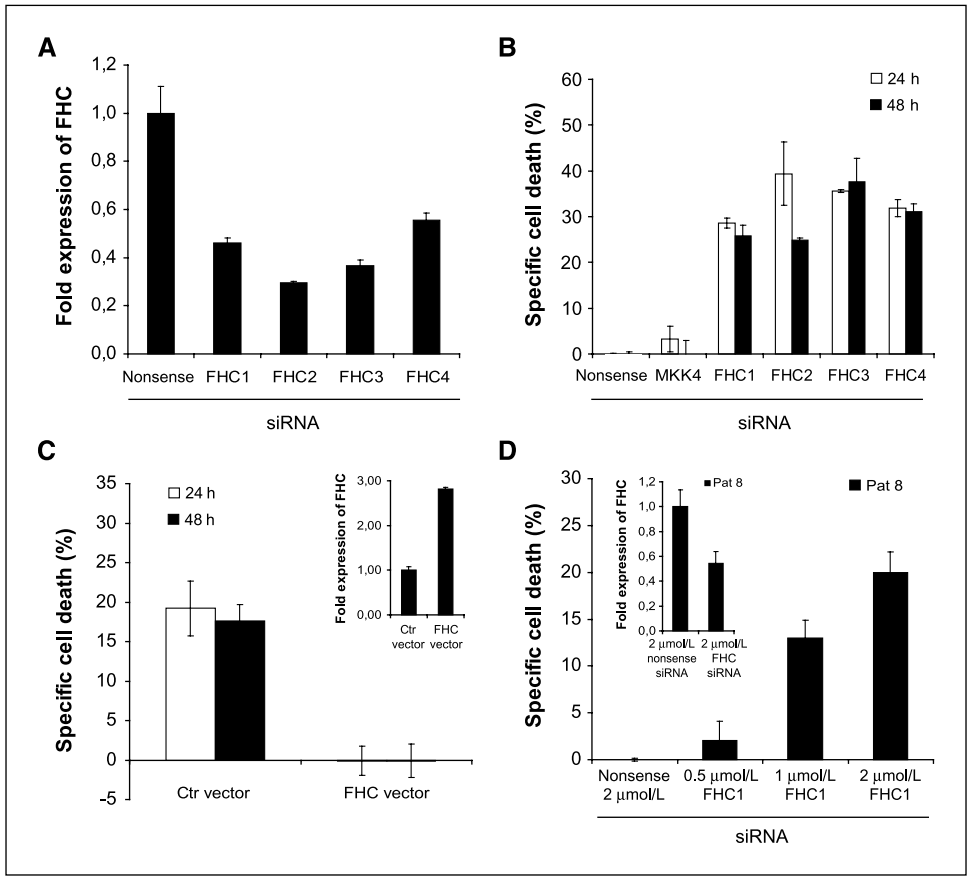


**Figure 4.** siRNA-mediated knockdown of FHC induces cell death in CTCL cell line and primary Sézary cells. *A,* knockdown of FHC by four different siRNAs was confirmed by quantitative RT-PCR after 24 h. *B,* MyLa cell line was treated with 1 μmol/L nonsense siRNA, 1 μmol/L MAP kinase kinase 4 siRNA, or 1 μmol/L of four different siRNAs targeted against FHC. Cell death was assessed by flow cytometry after 24 and 48 h. *C,* cells were transiently transfected either with control vector or a vector encoding the open reading frame FHC. Overexpression of FHC was assessed by quantitative RT-PCR (*insert*). FHC5 siRNA, targeting the 3′ UTR of FHC, was used to knock down FHC and cell death was analyzed after 24 and 48 h. *D,* purified T cells from patient 8 were transfected with FHC2 siRNA, and cell death of $V\beta1^+$ and $V\beta1^-$ T cells was analyzed after 24 h. Knockdown of FHC was assessed by RT-PCR (*insert*). The experiment shown is representative for three independent patients analyzed.

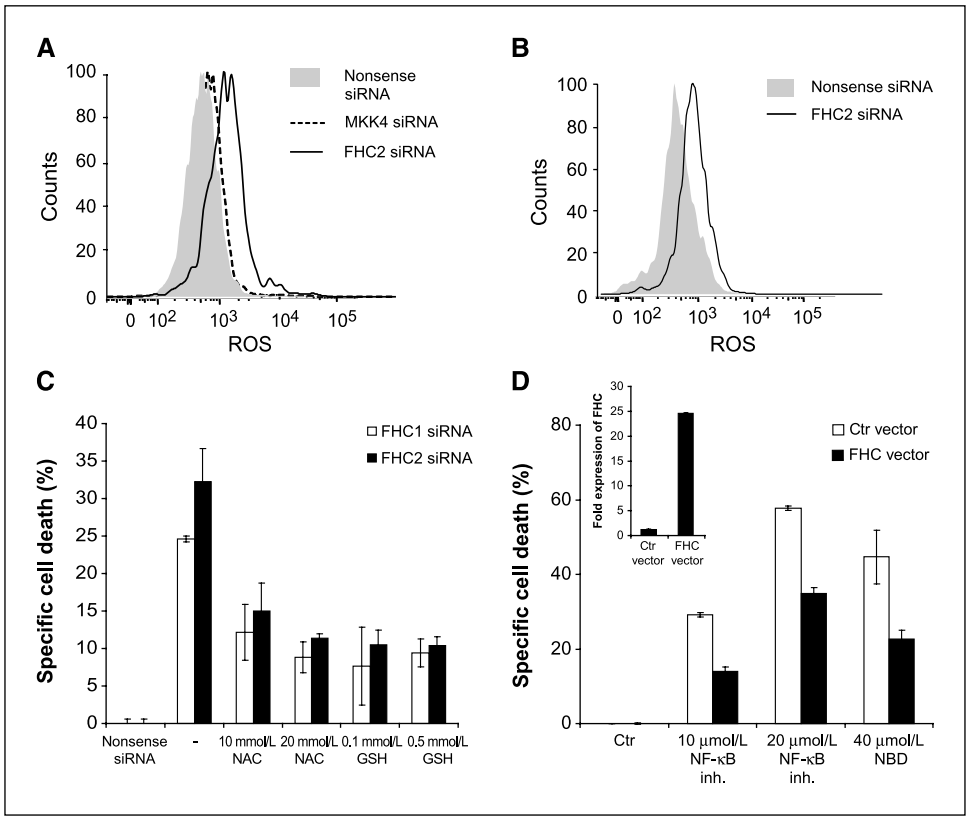


**Figure 5.** siRNA-mediated knockdown of FHC induces ROS in CTCL cell line and primary Sézary cells. *A,* MyLa cells were transfected with nonsense siRNA, MAP kinase kinase 4 siRNA, and FHC 2 siRNA. After 6 h of incubation with siRNA, cells were stained for 30 min with $H_2$DCFDA and the ROS generation was measured by flow cytometry. *B,* purified T cells from patient 3 were transfected with FHC2 siRNA. After 6 h of incubation with siRNA, cells were stained for 30 min with $H_2$DCFDA and the ROS generation was measured by flow cytometry. The experiment shown is representative for two independent patients analyzed. *C,* MyLa cells were transfected either with nonsense siRNA or two different siRNAs against FHC (*FHC1, FHC2*) and treated with the indicated concentrations of NAC or GSH. Cell death was assayed after 24 h. *D,* MyLa cells were transiently transfected with either vector or with a vector encoding for FHC. Positively transfected cells were sorted by flow cytometry and treated with the indicated concentrations of NF-κB inhibitor and NBD. Cell death was assayed after 24 h. Expression of FHC was assessed by RT-PCR (*insert*).

regulation of FHC expression by constitutively active NF-κB pathway is important for the survival of CTCL cells.

**Inhibition of NF-κB delays tumor growth *in vivo* by down-regulation of FHC expression.** To investigate whether manipulation of the intracellular free iron level can induce cell death in other T-cell tumors, we sought to analyze the effects of NF-κB inhibition in the T cell lymphoma RMA-S. RMA-S is a murine lymphoma cell line derived from the Rauscher MuLV-induced RBL-5 cell line (35). Inhibition of NF-κB induced a increase of LIP and ROS in RMA-S cells *in vitro* as observed for MyLa, Hut78, SeAx cells, or malignant T cells from Sézary patients (Supplementary Fig. S3*A*; Fig. 6*A*). Furthermore, FHC down-regulation *via* siRNA induced a ROS-dependent cell death that could be blocked by antioxidants (Fig. 6*B*). This shows that RMA-S cells react to inhibition of NF-κB in a similar way as MyLa, Hut78, SeAx cells, or primary patient cells. To analyze whether NF-κB activity and expression of FHC are required for tumor growth *in vivo*, $1 \times 10^6$ RMA-S cells were injected s.c. into C57BL/6 mice. In toxicity studies, 396 μg/kg of NF-κB inhibitor was found to be sublethal for C57BL/6 mice (data not shown). Therefore, mice were either mock treated or treated daily with 396 μg/kg NF-κB inhibitor beginning on day 6 after tumor cell injection. We observed that tumors of mice treated with NF-κB inhibitor grew at a significantly slower rate than in mock-treated mice (Fig. 6*C*). Mice were sacrificed and tumors were isolated on day 17. Tumors of mice treated with NF-κB inhibitor showed a significantly lower expression of FHC compared with mock-treated mice (Fig. 6*D*). Thus, FHC expression influences tumor growth *in vivo*. To estimate the general toxicity of *in vivo* application of the NF-κB inhibitor, animal weight was measured and no particular differences during treatment were observed (Supplementary Fig. S3*B*). Furthermore, the complete blood count of three mice of each treatment group showed comparable values for leukocytes, erythrocytes, haemoglobin, and thrombocytes (Supplementary Fig. S3*B*). Taken together, these experiments confirm the effect of FHC expression on tumor growth *in vivo*. NF-κB inhibition induces a down-modulation of FHC expression, which finally decreases tumor growth. Thus, interference with FHC expression levels seems to be a promising tool for treatment of lymphomas.

## Discussion

The present study shows that inhibition of the NF-κB pathway in lymphomas with constitutively activated NF-κB causes cell death, which is dependent on ROS and iron. Furthermore, the study defines FHC as an important target of constitutively active NF-κB in malignant T cells from patients with Sézary syndrome that is required for regulation of iron and ROS levels in cells.

FHC has been described as a target gene for NF-κB signaling induced by TNFα or Ras transformation (18, 36). However, here, we found that the FHC expression level is controlled by constitutively active NF-κB in malignant T cells without further stimuli. Remarkably, inhibition of NF-κB led to down-regulation of FHC in T cells from Sézary patients but not in T cells from normal healthy donors. In addition, an increase of the intracellular iron LIP was also exclusively observed for CTCL cell lines or T cells from Sézary patients but not in normal T cells. Finally, inhibition of NF-κB induced cell death in malignant T cells isolated from Sézary patients and CTCL cell lines but not in normal T cells. In conclusion, all events that are involved in cell death were only seen in malignant cells. Recent studies showed that constitutive activation of NF-κB is found in Sézary cells but not in T cells from normal healthy donors (12, 37). This might explain why

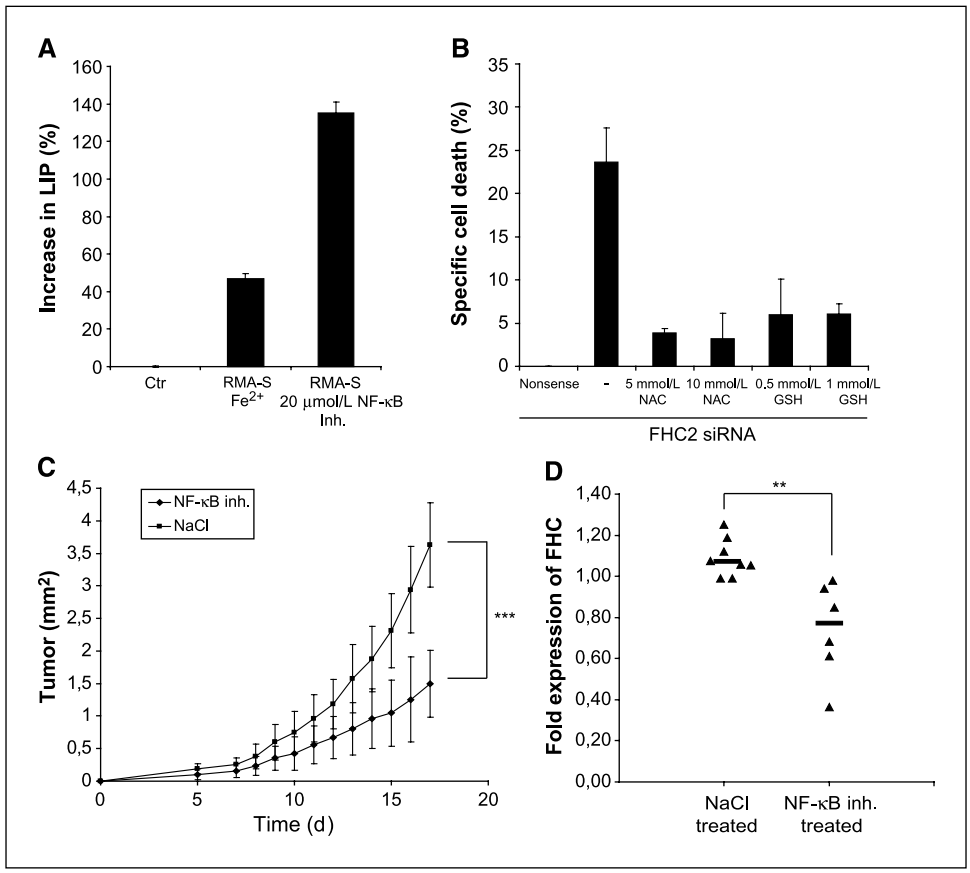


**Figure 6.** Inhibition of the NF-κB pathway delays tumor growth *in vivo*. *A,* RMA-S cells were incubated with 0.01 μmol/L calcein-AM for 30 min, either left untreated or treated with 20 μmol/L NF-κB inhibitor for 2 h. Then, all samples were treated with 100 μmol/L of iron chelator DP for 1 h. Fluorescence of calcein was measured by flow cytometry. *B,* RMA-S cells were transfected with 1 μmol/L nonsense siRNA or with 1 μmol/L FHC2 siRNA. 6 h after transfection cells were taken up in medium containing increasing concentrations of NAC or GSH. Cell death was analyzed after 24 h. *C,* $1 \times 10^6$ RMA-S cells were injected s.c. in C57BL/6 mice ($n = 14$ per group). Increase in tumor size was assayed beginning on day 5. Statistical significance was assessed by Koziol's test (50); ***, $P < 0.001$. Results shown are representative for two independent experiments. *D,* at day 17, 6 to 8 mice of each treatment group were sacrificed, tumor cells were isolated, and FHC expression levels were assessed by quantitative RT-PCR. Student's *t* test, $P < 0.01$ (**).

inhibition of NF-κB is more toxic to Sézary cells but not to normal T cells and might render NF-κB or FHC promising drug candidates without severe side effects.

Inhibition of the NF-κB pathway results in an increase of iron, which in consequence catalyzes a massive generation of ROS *via* the Fenton reaction. Cell death caused by this strong oxidative stress can be blocked by FHC overexpression and iron chelators such as DFO. This shows that FHC acts protective and antiapoptotic in cancers with constitutive NF-κB signaling. An increase of ROS was also observed when FHC was targeted directly by siRNA, which induced cell death of MyLa cells and malignant T cells from patients with Sézary syndrome. Down-regulation of FHC causes an increase in free intracellular iron. Free iron participates in the Fenton reaction generating hydroxyl radicals and hydroxide anions from hydrogen peroxide (19). Hydroxyl radicals are highly reactive and react with a variety of biological molecules including DNA, RNA, cholesterol, lipids, carbohydrates, and proteins. The extent of damage to particular targets depends on a number of factors including the concentration of the target, the rate constant for the reaction of the oxidant with the target, the location of the target when compared with the side of radical formation, the occurrence of secondary damaging events (chain reactions and damage transfer processes), the occurrence of oxidant-scavenging reactions, and repair reactions. Hydroxyl radicals can react with the backbone of proteins and amino acid side chains resulting in the formation of further damaging reactive species. These reactive species can induce damage to other biomolecules including lipids and other proteins in a chain reaction like manner (20). Low amounts of ROS, especially less reactive and more selective molecules such as $H_2O_2$, can act as second messengers for proper development, proliferation, and apoptosis regulation (26, 27, 38). High amounts of ROS, especially highly reactive and less specific molecules such as hydrogen peroxide, lead to induction of oxidative stress, cell death, and aging (34). Here, we show that an increase of free iron led to generation of massive oxidative stress and cell death in CTCL cell lines and T cells from Sézary patients. It is known that massive cellular oxidation by strong generation of ROS may lead to necrotic cell death instead of apoptosis (39). This is supported by our observation that inhibitors of classic cell death pathways or caspase inhibitor zVAD were not effective at suppressing cell death. Thus, investigated cell death is different from classic apoptosis and rather might be necrotic.

The proteasome inhibitor bortezomib is widely used as NF-κB inhibitor because it blocks degradation of IkBα. However, we observed that bortezomib induced only a mild oxidative stress, which was independent of iron (data not shown). This suggests that FHC is not down-regulated by bortezomib, likely because bortezomib blocks degradation of FHC by the proteasome and thus, interferes with FHC degradation. In conclusion, bortezomib does not cover all events of NF-κB inhibition and development of other NF-κB inhibitors or molecules targeting FHC are required.

FHC might be targeted in several ways. First, FHC shows enzymatic activity required for the storage of iron (III), the nontoxic form of iron for cells. Blocking this enzymatic activity by small-molecule inhibitors would abolish the capability for tumor cells to store iron in a secure way. Another option for FHC down-regulation comprises delivery of specific siRNA or miRNA into tumor cells. Decreased expression of FHC is of disadvantage

for growing cells and clearly blocked cell proliferation as evidenced by our *in vivo* model. Last, the uptake of iron into cells can be disrupted by antibodies specific for the transferrin receptor (CD71). Assuming that fast growing cells require enhanced iron uptake, antibodies blocking CD71 and thus interfering with iron uptake will delay cell proliferation.

Interference with FHC expression or down-regulation of FHC may occur at different kinetics. Fast down-regulation of FHC results in an immediate increase of free intracellular iron, which in turn results in massive generation of ROS and ultimately leads to cell death. Our data indicate that this oxidative stress might be more harmful to cancer cells because they generally show higher basic levels of ROS due to high energy demand and fast proliferation (40, 41). Slow and mild down-regulation of FHC is less toxic to cells but will deplete intracellular iron stores, thus decreasing proliferation rates (42). To investigate whether depletion of intracellular iron stores decreases tumor growth, we analyzed the effects of NF-κB inhibition *in vivo*. The murine T-lymphoma cell line RMA-S reacted absolutely comparable toward the NF-κB inhibitor as primary T cells from patients, or the three CTCL cell lines. This suggested the RMA-S model as a suitable system to investigate the NF-κB inhibitor *in vivo*. Furthermore, transplanting SeAx cells in immuno-deficient mice failed, and thus far, only a mouse model for mycosis fungoides was established (43). RMA-S cells were injected into C57BL/6 mice and mice were then treated with the NF-κB inhibitor. Inhibition of NF-κB caused down-regulation of FHC and significantly reduced tumor growth *in vivo*. This mechanism might be dependent on the tumor type and especially relevant for T-cell tumors because one previous report has described that a FHC knockdown had no effect on proliferation of HeLa cells *in vitro* (44). However, another report showed that FHC is involved in proliferation of the breast cell line MCF-7 (45). It is well-known that proliferating cells are strongly dependent on continuous iron supply for enzymes involved in DNA synthesis such as ribonucleotide reductase (46). Because iron is necessary for cellular proliferation, its depletion leads to cell cylce arrest, apoptosis, and delayed tumor growth *in vivo* (47, 48). We assume that constitutive NF-κB activation is required for fast-growing tumor cells to provide sufficient iron storage capacity for iron-dependent enzymes involved in proliferation.

Overexpression of FHC rescued ~50% of the cells treated with NF-κB inhibitor from cell death, suggesting that other targets of NF-κB may also play a role in this process. Recent data showed that alterations of Bcl-2 family members may be involved in induction of cell death. In CTCL cell lines treated with an IKK2 inhibitor, an up-regulation of proapoptotic Bax dimers and an down-regulation of survivin was reported (37). Whether alterations in expression are causative for cell death was not yet investigated (37).

An important message from our study is that regulation of FHC by constitutively active NF-κB signaling plays a major role for cell proliferation and apoptosis resistance in hematopoietic malignancies. This observation may also be important for the treatment of other cancers. Constitutive activation of NF-κB is well-described in other cancers including breast cancer or hepatocellular carcinoma (49). Thus, targeting intracellular iron homeostasis with NF-κB inhibitors or directly by specific inhibitors of proteins involved in iron metabolism, such as FHC, might be an attractive possibility for cancer treatment.

## Disclosure of Potential Conflicts of Interest

No potential conflicts of interest were disclosed.

## Acknowledgments

Received 8/19/2008; revised 11/18/2008; accepted 12/7/2008; published OnlineFirst 3/3/09.

**Grant support:** "Wilhelm Sander Stiftung" (2004.064.1/2007.126.1), "Network Aging Research - NAR" (Landesstiftung 6477.1), the Deutsche Forschungsgemeinschaft (DFG, 405/4-2006), the Helmholtz Alliance Immunotherapy of Cancer and the EU.

The costs of publication of this article were defrayed in part by the payment of page charges. This article must therefore be hereby marked *advertisement* in accordance with 18 U.S.C. Section 1734 solely to indicate this fact.

We thank the patients with Sézary syndrome for blood donations, D. Süss, M. Becker, S. Pfrang, C. Quirin, and E. Frey for technical assistance; J. Hoffmann, R. Arnold, D. Brenner, and M. Brechmann for critical reading of the manuscript; and A. Cerwenka, L. Edler, and S. Goerdt for support.

## References

1. Braun T, Carvalho G, Fabre C, Grosjean J, Fenaux P, Kroemer G. Targeting NF-κB in hematologic malignancies. Cell Death Differ 2006;13:748–58.
2. Golks A, Brenner D, Krammer PH, Lavrik IN. The c-FLIP-NH2 terminus (p22-FLIP) induces NF-κB activation. J Exp Med 2006;203:1295–305.
3. Karin M. Nuclear factor-κB in cancer development and progression. Nature 2006;441:431–6.
4. Annunziata CM, Davis RE, Demchenko Y, et al. Frequent engagement of the classical and alternative NF-κB pathways by diverse genetic abnormalities in multiple myeloma. Cancer Cell 2007;12:115–30.
5. Keats JJ, Fonseca R, Chesi M, et al. Promiscuous mutations activate the noncanonical NF-κB pathway in multiple myeloma. Cancer Cell 2007;12:131–44.
6. Davis RE, Brown KD, Siebenlist U, Staudt LM. Constitutive nuclear factor κB activity is required for survival of activated B cell-like diffuse large B cell lymphoma cells. J Exp Med 2001;194:1861–74.
7. Frelin C, Imbert V, Griessinger E, et al. Targeting NF-κB activation via pharmacologic inhibition of IKK2-induced apoptosis of human acute myeloid leukemia cells. Blood 2005;105:804–11.
8. Weston VJ, Austen B, Wei W, et al. Apoptotic resistance to ionizing radiation in pediatric B-precursor acute lymphoblastic leukemia frequently involves increased NF-κB survival pathway signaling. Blood 2004; 104:1465–73.
9. Hamdane M, David-Cordonnier MH, D'Halluin JC. Activation of p65 NF-κB protein by p210BCR-ABL in a myeloid cell line (P210BCR-ABL activates p65 NF-κB). Oncogene 1997;15:2267–75.
10. Carvalho G, Fabre C, Braun T, et al. Inhibition of NEMO, the regulatory subunit of the IKK complex, induces apoptosis in high-risk myelodysplastic syndrome and acute myeloid leukemia. Oncogene 2007;26: 2299–307.
11. Fabre C, Carvalho G, Tasdemir E, et al. NF-κB inhibition sensitizes to starvation-induced cell death in high-risk myelodysplastic syndrome and acute myeloid leukemia. Oncogene 2007;26:4071–83.
12. Sors A, Jean-Louis F, Pellet C, et al. Down-regulating constitutive activation of the NF-κB canonical pathway overcomes the resistance of cutaneous T-cell lymphoma to apoptosis. Blood 2006;107:2354–63.
13. Thakur S, Lin HC, Tseng WT, et al. Rearrangement and altered expression of the NFKB-2 gene in human cutaneous T-lymphoma cells. Oncogene 1994; 9:2335–44.
14. Willemze R, Jaffe ES, Burg G, et al. WHO-EORTC classification for cutaneous lymphomas. Blood 2005;105: 3768–85.
15. Klemke CD, Mansmann U, Poenitz N, Dippel E, Goerdt S. Prognostic factors and prediction of prognosis by the CTCL Severity Index in mycosis fungoides and Sezary syndrome. Br J Dermatol 2005; 153:118–24.
16. Brenner D, Golks A, Kiefer F, Krammer PH, Arnold R. Activation or suppression of NFκB by HPK1 determines sensitivity to activation-induced cell death. EMBO J 2005;24:4279–90.
17. Kamata H, Honda S, Maeda S, Chang L, Hirata H, Karin M. Reactive oxygen species promote TNFα-induced death and sustained JNK activation by inhibiting MAP kinase phosphatases. Cell 2005;120:649–61.
18. Pham CG, Bubici C, Zazzeroni F, et al. Ferritin heavy chain upregulation by NF-κB inhibits TNFα-induced apoptosis by suppressing reactive oxygen species. Cell 2004;119:529–42.
19. Torti FM, Torti SV. Regulation of ferritin genes and protein. Blood 2002;99:3505–16.
20. Davies MJ. The oxidative environment and protein damage. Biochim Biophys Acta 2005;1703:93–109.
21. Ferreira C, Bucchini D, Martin ME, et al. Early embryonic lethality of H ferritin gene deletion in mice. J Biol Chem 2000;275:3021–4.
22. Hentze MW, Kuhn LC. Molecular control of vertebrate iron metabolism: mRNA-based regulatory circuits operated by iron, nitric oxide, and oxidative stress. Proc Natl Acad Sci U S A 1996;93:8175–82.
23. Picard V, Epsztejn S, Santambrogio P, Cabantchik ZI, Beaumont C. Role of ferritin in the control of the labile

iron pool in murine erythroleukemia cells. J Biol Chem 1998;273:15382–6.
24. Epsztejn S, Glickstein H, Picard V, et al. H-ferritin subunit overexpression in erythroid cells reduces the oxidative stress response and induces multidrug resistance properties. Blood 1999;94:3593–603.
25. Orino K, Lehman L, Tsuji Y, Ayaki H, Torti SV, Torti FM. Ferritin and the response to oxidative stress. Biochem J 2001;357:241–7.
26. Kaminski M, Kiessling M, Suss D, Krammer PH, Gulow K. Novel role for mitochondria: protein kinase Ctheta-dependent oxidative signaling organelles in activation-induced T-cell death. Mol Cell Biol 2007;27:3625–39.
27. Gulow K, Kaminski M, Darvas K, Suss D, Li-Weber M, Krammer PH. HIV-1 trans-activator of transcription substitutes for oxidative signaling in activation-induced T cell death. J Immunol 2005;174:5249–60.
28. Epsztejn S, Kakhlon O, Glickstein H, Breuer W, Cabantchik I. Fluorescence analysis of the labile iron pool of mammalian cells. Anal Biochem 1997;248:31–40.
29. Walczak H, Sprick MR. Biochemistry and function of the DISC. Trends Biochem Sci 2001;26:452–3.
30. Tobe M, Isobe Y, Tomizawa H, et al. Discovery of quinazolines as a novel structural class of potent inhibitors of NF-κ B activation. Bioorg Med Chem 2003;11:383–91.
31. Jimi E, Aoki K, Saito H, et al. Selective inhibition of NF-κ B blocks osteoclastogenesis and prevents inflammatory bone destruction *in vivo*. Nat Med 2004;10:617–24.
32. Schwab C, Willers J, Niederer E, et al. The use of anti-T-cell receptor-Vβ antibodies for the estimation of treatment success and phenotypic characterization of clonal T-cell populations in cutaneous T-cell lymphomas. Br J Haematol 2002;118:1019–26.
33. Allen RG, Tresini M. Oxidative stress and gene regulation. Free Radic Biol Med 2000;28:463–99.
34. Finkel T, Holbrook NJ. Oxidants, oxidative stress and the biology of ageing. Nature 2000;408:239–47.
35. Karre K, Ljunggren HG, Piontek G, Kiessling R. Selective rejection of H-2-deficient lymphoma variants suggests alternative immune defence strategy. Nature 1986;319:675–8.
36. Duran A, Linares JF, Galvez AS, et al. The signaling adaptor p62 is an important NF-κB mediator in tumorigenesis. Cancer Cell 2008;13:343–54.
37. Sors A, Jean-Louis F, Begue E, et al. Inhibition of IκB kinase subunit 2 in cutaneous T-cell lymphoma down-regulates nuclear factor-κB constitutive activation, induces cell death, and potentiates the apoptotic response to antineoplastic chemotherapeutic agents. Clin Cancer Res 2008;14:901–11.
38. Roth S, Droge W. Regulation of T-cell activation and T-cell growth factor (TCGF) production by hydrogen peroxide. Cell Immunol 1987;108:417–24.
39. Higuchi Y. Chromosomal DNA fragmentation in apoptosis and necrosis induced by oxidative stress. Biochem Pharmacol 2003;66:1527–35.
40. Schumacker PT. Reactive oxygen species in cancer cells: live by the sword, die by the sword. Cancer Cell 2006;10:175–6.
41. Szatrowski TP, Nathan CF. Production of large amounts of hydrogen peroxide by human tumor cells. Cancer Res 1991;51:794–8.
42. Pahl PM, Horwitz LD. Cell permeable iron chelators as potential cancer chemotherapeutic agents. Cancer Invest 2005;23:683–91.
43. Thaler S, Burger AM, Schulz T, et al. Establishment of a mouse xenograft model for mycosis fungoides. Exp Dermatol 2004;13:406–12.
44. Cozzi A, Corsi B, Levi S, Santambrogio P, Biasiotto G, Arosio P. Analysis of the biologic functions of H- and L-ferritins in HeLa cells by transfection with siRNAs and cDNAs: evidence for a proliferative role of L-ferritin. Blood 2004;103:2377–83.
45. Yang DC, Wang F, Elliott RL, Head JF. Expression of transferrin receptor and ferritin H-chain mRNA are associated with clinical and histopathological prognostic indicators in breast cancer. Anticancer Res 2001;21:541–9.
46. Nyholm S, Mann GJ, Johansson AG, Bergeron RJ, Graslund A, Thelander L. Role of ribonucleotide reductase in inhibition of mammalian cell growth by potent iron chelators. J Biol Chem 1993;268:26200–5.
47. Hann HW, Stahlhut MW, Rubin R, Maddrey WC. Antitumor effect of deferoxamine on human hepatocellular carcinoma growing in athymic nude mice. Cancer 1992;70:2051–6.
48. Lederman HM, Cohen A, Lee JW, Freedman MH, Gelfand EW. Deferoxamine: a reversible S-phase inhibitor of human lymphocyte proliferation. Blood 1984;64:748–53.
49. Sethi G, Sung B, Aggarwal BB. Nuclear factor-κB activation: from bench to bedside. Exp Biol Med (Maywood) 2008;233:21–31.
50. Koziol JA, Maxwell DA, Fukushima M, Colmerauer ME, Pilch YH. A distribution-free test for tumor-growth curve analyses with application to an animal tumor immunotherapy experiment. Biometrics 1981;37:383–90.